UNCLASSIFIED

AD 278 575

Reproduced
by the

ARMED SERVICES TECHNICAL INFORMATION AGENCY
ARLINGTON HALL STATION
ARLINGTON 12, VIRGINIA

UNCLASSIFIED

REPRODUCED FROM
BEST AVAILABLE COPY

NOTICE: When government or other drawings, specifications or other data are used for any purpose other than in connection with a definitely related government procurement operation, the U. S. Government thereby incurs no responsibility, nor any obligation whatsoever; and the fact that the Government may have formulated, furnished, or in any way supplied the said drawings, specifications, or other data is not to be regarded by implication or otherwise as in any manner licensing the holder or any other person or corporation, or conveying any rights or permission to manufacture, use or sell any patented invention that may in any way be related thereto.

278575 CATALOGED BY ASTIA AS AD No. 278575

USL Report No. 550
1-405-00-00

COLOSSUS II SHALLOW-WATER ACOUSTIC PROPAGATION STUDIES

(SS046002-8037)

1 June 1962

U. S. NAVY UNDERWATER SOUND LABORATORY
FORT TRUMBULL NEW LONDON, CONNECTICUT

FOREWORD

The material presented in this report appeared earlier as a portion of USL Report No. 513, Colossus II Summary Report (U) dated 3 July 1961. The complete report No. 513 is classified. The purpose of this report is to permit the propagation information in Report No. 513 to appear in the unclassified literature.

The reduction and analysis of the data were done by the Crosley Division of Avco Corporation under Contract N140(70024)67165B with the Underwater Sound Laboratory. R. W. Hasse, Jr., and R. A. Westervelt, both of USL, provided technical consultations. All the data analyzed were provided by the Laboratory.

ABSTRACT

Project Colossus II was established in 1954 to investigate acoustics in shallow water (150 fathoms or less). A portion of that program was devoted to a study of underwater acoustic propagation. The frequency range of interest was 100 to 3000 cps.

Presented in this report are the results of the acoustic propagation loss studies, which include a summary of the analysis and a prediction method of estimating the statistical distribution of propagation loss.

ADMINISTRATIVE INFORMATION

Work on the Colossus II program was accomplished under Navy Project and Task No. SS046002-8037 and USL Project No. 1-500-00-00. This latter project has been terminated and the program is now included under USL Project No. 1-405-00-00.

REVIEWED AND APPROVED: 1 June 1962

J. Warren Horton
Technical Director

B. H. Andrews, Captain, USN
Commanding Officer and Director

TABLE OF CONTENTS

LIST OF ILLUSTRATIONS

LIST OF TABLES

COLOSSUS II SHALLOW-WATER ACOUSTIC PROPAGATION STUDIES

INTRODUCTION

This report covers the Colossus II study of shallow-water acoustic propagation loss data. The reduction and analysis of the data were done by the Crosley Division of Avco Corporation under Contract N140(70024)67165B with the Underwater Sound Laboratory. R. W. Hasse, Jr., and R. A. Westervelt, both of USL, provided technical consultations. All the data analyzed were provided by the Laboratory.

The bulk of the measurements was made by the Laboratory in the period since 1955. Although coverage represented by the data is incomplete, the entire collection now available in the shallow-water file represents a degree of completeness not likely to be improved for many years. The Underwater Sound Laboratory Colossus data are supplemented by data from MEDEA, ARL, WHOI, CUDWR, and UCDWR.

Presented are summaries of the analysis, the status of the shallow-water file, and a complete prediction method of estimating the statistical distribution of propagation loss.

No theoretical treatment of the data has been made, the prediction method being semi-empirical, largely equivalent to that used in Project AMOS. The validity of the method depends on its consistency, reasonableness, and utility in representing the available data.

The processed Acoustic Data Sources are listed later in the report. Other documents were received, but owing to lack of information they could not be processed. A complete bibliography of the Acoustic Data Sources appears in USL Report No. 513 (CONFIDENTIAL).

DESCRIPTION OF SHALLOW-WATER PROPAGATION

A number of formulas and charts are presented with summarize the existing shallow-water propagation data for acoustic frequencies from 100 cps to 2820 cps and which can be extended to higher frequencies. The major source of data for this purpose came from the Colossus II program being carried out by the Underwater Sound Laboratory. During the years 1956 to the present, large quantities of propagation loss data and reverberation data were obtained, mostly with explosive sources, but

also with underwater sirens and sinusoidal acoustic generators, off the East Coast of the United States. The shots were recorded on magnetic tape and analyzed in logit frequency bands from 70 cps to 2820 cps. Measurements were made at various projector and receiver depths at ranges out to 50 miles or more.

The point of departure for the present study was the Project AMOS analysis at higher frequencies in deep water and recently completed studies of surface scattering loss in isothermal layers. The propagation loss data over the frequency range from 100 cps to 3000 cps were analyzed and interpreted according to a definite model compatible with the AMOS analysis. Equations of propagation loss were fitted with semi-empirical coefficients. The steps used to arrive at this model were:

b. Studying acoustic patterns in situations where one of these variables is dominant.

c. Making the simplest assumptions regarding the acoustic interrelation of these variables and adding complications only when necessary to incorporate a large body of data into the model.

d. Requiring that the model be self-consistent with the AMOS analysis and the subsequent lower-frequency, deep-water analysis based on sea-surface scattering.

Propagation Data Analysis

The analysis, then, consisted of finding the most important variables occurring in the shallow-water propagation-loss data. There was no doubt that range and frequency were the two most important variables. The propagation loss increased with frequency above 100 cps. One would also expect the loss to increase with range following a 20 log R law out to some range which could vary from one situation to another, and then follow some different relationship as boundary effects and absorption became more important. The hypothesis was made to define skip distance (H) in such a way that H represents the maximum range at which rays first make contact with either the sea surface or bottom.

It was shown in the Project Amos analysis that:

$$H = 0.5\sqrt{L} \text{ kyd for upward refraction in isothermal water} \quad (1A)$$

and

$$H = 0.4\sqrt{D} \text{ kyd for downward refraction in average negative gradient water} \quad (1B)$$

where

L is the layer depth in feet and

D is the water depth in feet.

The study was concerned for the most part with measurements made using explosives. For converting received levels into propagation loss a first approximation was made that the best estimation of explosive source levels might be realized by assuming square law spreading to a nominal range (usually 3000 yards).

The data were then fitted to the form:

$$N_w = 20 \log_{10} R + aR + 60 \text{ (db)} \qquad R \leq H \qquad (2A)$$

$$N_w = 10 \log_{10} R + 10 \log_{10} H + aR + a_T' (R - H) + 60 \text{ (db)} \qquad R \geq H \qquad (2B)$$

where

R is the range in kyds,

$a = 0.01 f^2$ db/kyd (average absorption coefficient for low frequencies),

f is the frequency in kc, and

a_T' is the residual shallow-water propagation loss factor, db/kyd. (This varies from one situation to another.)

This varies from one situation to another.

Skip Distance as a Scaling Parameter

The residual propagation loss factor a_T' is then characteristic of shallow water propagation and is a function of frequency, bottom type, sea state, water depth, projector depth, receiver depth, sound speed structure, and other variables. In studying the dependence of the propagation loss on environmental factors, it would be extremely helpful to have a scale factor which would increase the effective number of measurements and replace range and water depth as descriptive variables. The skip distance (H) was found to apply in isothermal layer propagation and was natural to try in this case. By dividing H into the range (R) we obtain an effective number of bottom and surface contacts which control the loss along a limiting ray. The propagation loss is then controlled by those rays having the smallest number of bottom and surface contacts. The skip distance concept normalizes the effects of

the bottom and sea surface on a "per contact" or "per bounce" basis. Thus, setting $R/H = n$ in Eq. (2B) we arrive at:

$$N_w = 20 \log_{10} R + aR + 60 \text{ (db)} \qquad R \leq H \qquad (3A)$$

$$N_w = 10 \log_{10} R + 10 \log_{10} H + aR + a_T (n - 1) + 60 \text{ (db)} \qquad R \geq H \qquad (3B)$$

where

a_T is the shallow-water attenuation constant on a per bounce basis.

Actually, the transition from spherical to cylindrical spreading should occur over several zones. The data indicate that this transition is complete by the ninth zone. Taking an intermediate value for spreading during transition, we have finally Eqs. (4A), (4B), and (4C).

$$N_w = 20 \log_{10} R + aR + 60 \text{ (db)} \qquad R \leq H \qquad (4A)$$

$$= 15 \log_{10} R + aR + a_T \left(\frac{R}{H} - 1 \right) + 5 \log_{10} H + 60 \text{ (db)} \qquad 8H \geq R \geq H \qquad (4B)$$

$$= 10 \log_{10} R + aR + a_T \left(\frac{R}{H} - 1 \right) + 10 \log_{10} H + 64.5 \text{ (db)} \qquad R \geq 8H \qquad (4C)$$

Effect of Thermal Structure

The data showed a strong increase in propagation loss in summer compared with winter. Since the sound speed gradients were negative to the bottom in the summer and positive to the bottom in winter, we were able to compute quite definite skip distances for both these situations from Eqs. (1A) and (1B). For the case where the layer depth is less than the water depth, the following approximate expression was used to compute the skip distance of the limiting ray:

$$H = \sqrt{\frac{L + D}{8}} \text{ kyd.} \qquad (5)$$

Eq. (5) gives a smaller H if $L = 0$ than does Eq. (1B) and represents the shallow-water data better.

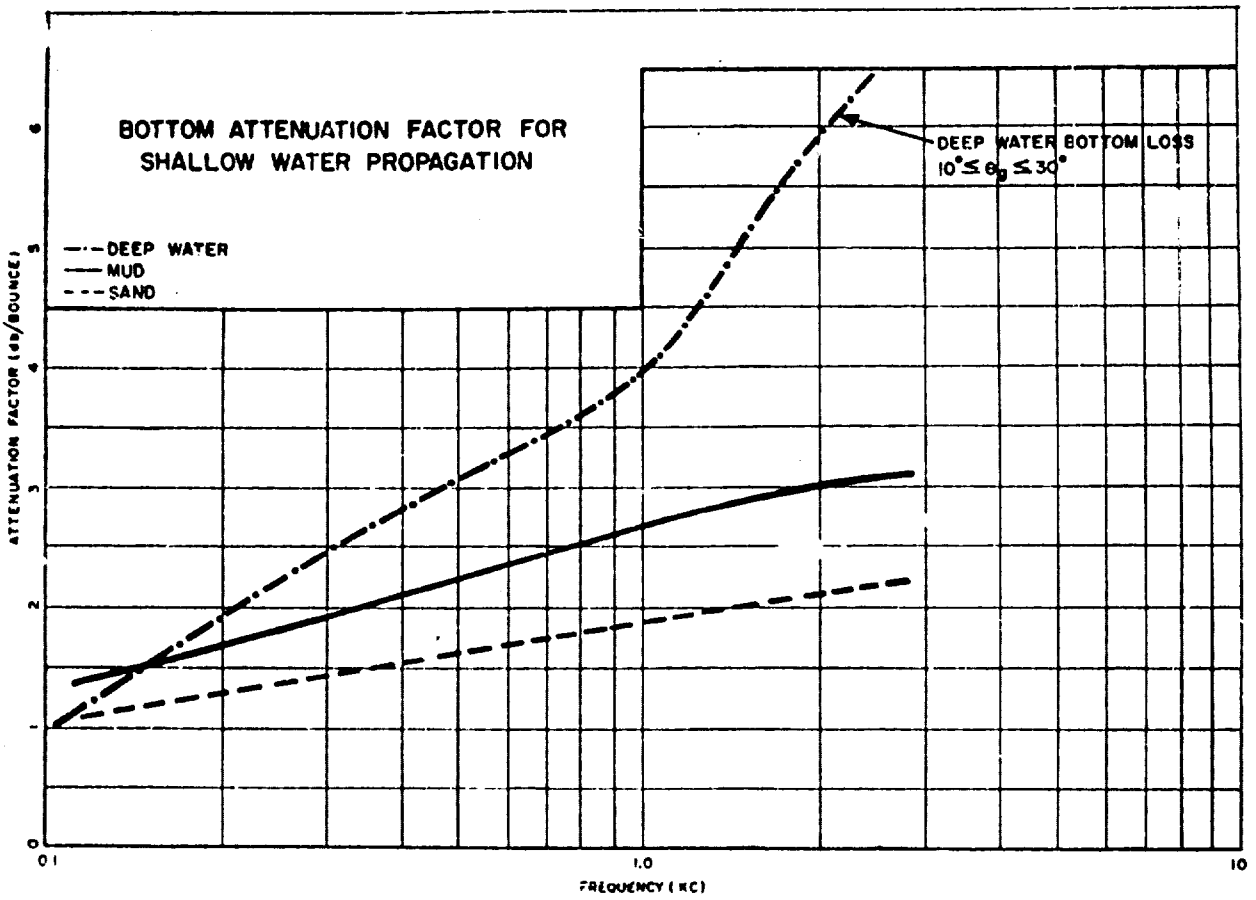

Fig. 1 - Bottom Attenuation Factor for Shallow Water Propagation

Effect of Bottom Type

Since the sea states were almost always low in the summer, it was possible to compare the loss per bounce for sea state 0 over mud and over sand. These two were the principal bottom types. Figure 1 shows the results. It is seen that the bottom loss for sand bottoms is appreciably less than that for mud bottoms, as expected. It may also be seen that these results are compatible with the deep-water bottom losses as reported in project AMOS for grazing between 10° and 30°.

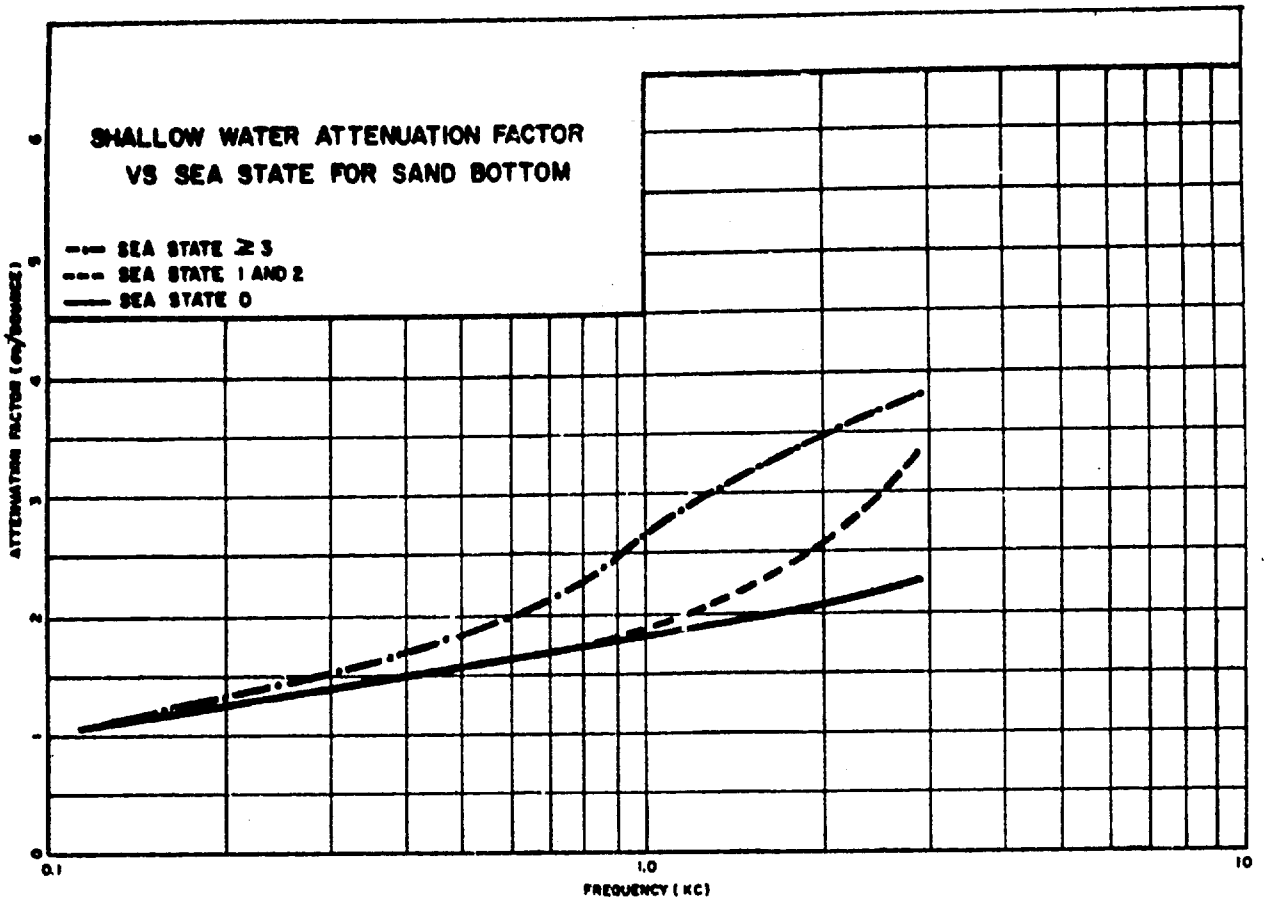

Fig. 2 - Shallow-Water Attenuation Factor vs Sea State for Sand Bottom

Effect of Sea State

In Fig. 2, the effect of sea state is demonstrated for the winter data. In this case where upward refraction occurs, it is expected that the sea state would have a strong influence on the propagation. Actually, the loss per contact looks like the bottom loss (most of the measurements were made over sand) rather than like the sea surface loss shown in Fig. 3. The surface scattering loss has a much larger frequency dependence. For example, this may be seen by setting the mean wave height equal to 1 foot (sea state 0-1) in the product of frequency and mean wave height. This behavior with sea state might be expected if most of the energy scattered from the surface is reflected by the bottom and returned for propagation down the channel. In deep water, a_s measures the energy which is scattered out of the surface channel and which is either lost in absorption on the way to the bottom or absorbed in the bottom through high grazing angle incidence.

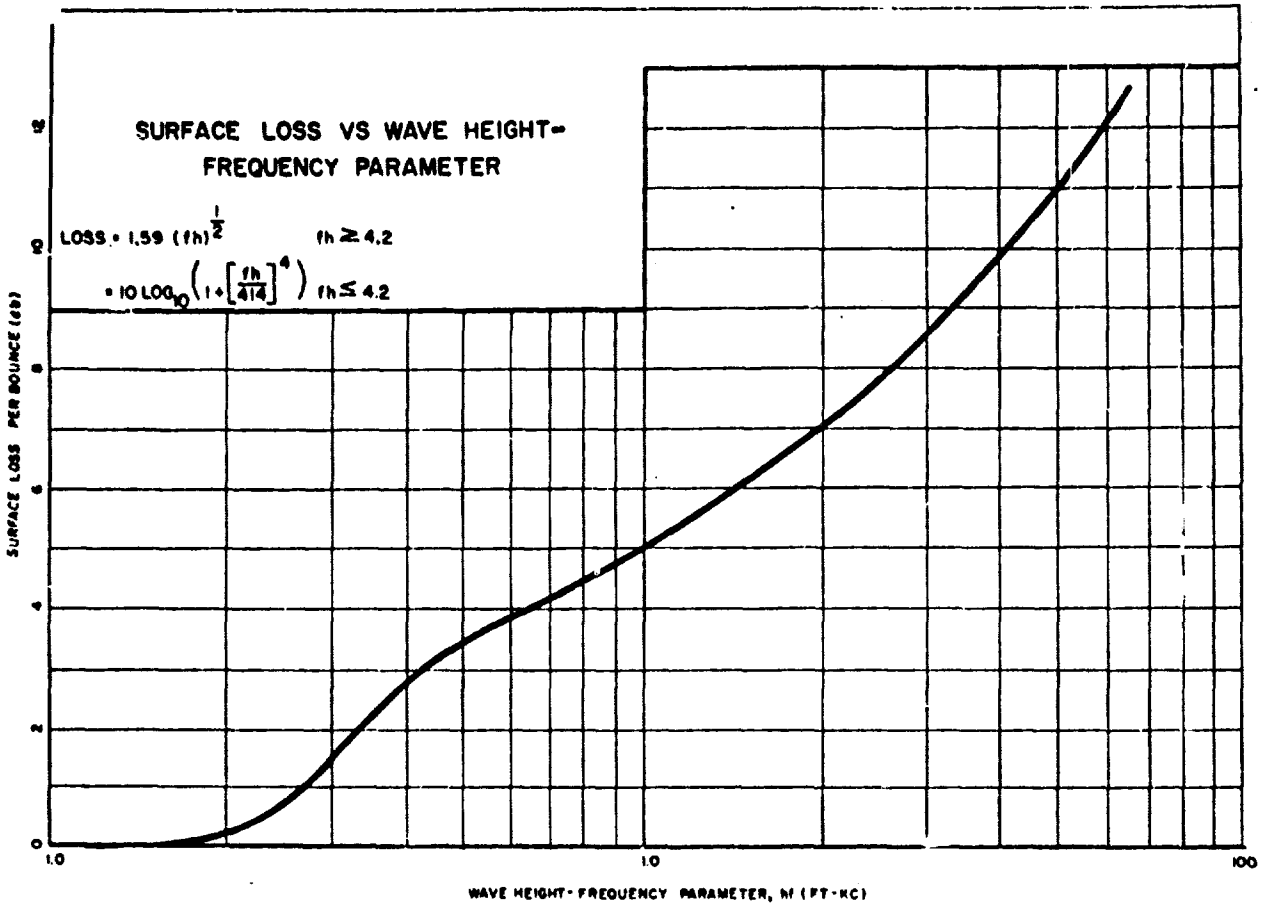

Fig. 3 - Surface Loss vs Wave Height-Frequency Parameter

Surface-Bottom Coupling

The problem then is to determine the extent of the coupling between this surface and the bottom from the measurements data of Fig. 2 for sea state 0, sea states 1 and 2, and sea states 3 and greater. If r_s is the surface reflection coefficient, then $(1 - r_s)$ is the surface scattering coefficient and $a_s = -10 \log_{10} r_s$ is the surface loss in db/bounce. The surface components r_s and $(1 - r_s)$ must suffer different interactions with the bottom if any sea state dependence is exhibited. We would expect scattered rays to suffer greater loss because they are steeper. The simplest expression satisfying this requirement and the observed data was:

$$r_t = r_s r_b + (1 - r_s) r_b^2$$

where

r_t is the fraction of energy transmitted down the channel when a bottom event is coupled with each surface reflection.

$a_t = -10 \log_{10} r_t$ (shallow-water attenuation constant, db/bounce).

r_b is the bottom reflection coefficient for the angles of incidence occurring in shallow water and is given in Fig. 1 for sand and for mud bottoms. ($a_b = -10 \log_{10} r_b$).

The observed behavior for a_t has profound significance on the interpretation of the shallow-water propagation mechanism. The fact that the grazing angle rays represented by r_s must be multiplied by r_b indicates that there is a bottom loss suffered by near-grazing rays. The fact that the scattered rays must be multiplied by r_b^2 means that the angular dependence of bottom reflection loss is such that these steeper rays suffer twice the loss of the near grazing rays.

Interpretation of Bottom Loss at Small Grazing Angles

The observed bottom loss at small grazing angles seems to imply a mode-changing process that takes energy for a refracted ray system and converts it to a simple bottom and surface bounce mode at great ranges. This is equivalent to the normal mode treatment of propagation in shallow water. This mode-changing process seems to occur for any sound speed structure. The sound speed structure determines the skip-distance zones. It would appear that after the first few zones, the skip-distance has a purely local significance representing a limiting free path for rays which happened to be scattered into grazing angles at that range. If, as is shown in the data, grazing rays must suffer one bottom contact loss per skip zone, then they can not be continuous from one zone to another. The possibility that horizontal rays suffer a bottom loss is hardly conceivable. The transition from one propagation mode to the other probably occurs over several skip zones, and we have adopted the convenient model that it occurs over the first eight skip zones. (See Eqs. (4A), (4B), and (4C).)

Near Field Considerations

Results of USL CW measurements indicated that at the short ranges, propagation was consistently superior to inverse square spreading. These results are consistent with other shallow-water data. In addition, several studies conducted at USL have shown average agreement between propagation studies made with CW and with explosive sources. Thus, it would appear that explosive source levels based on published data are satisfactory for converting from received levels to propagation loss. The departure of propagation loss in the near field from square law spreading can be accounted for by taking into account reflections in the

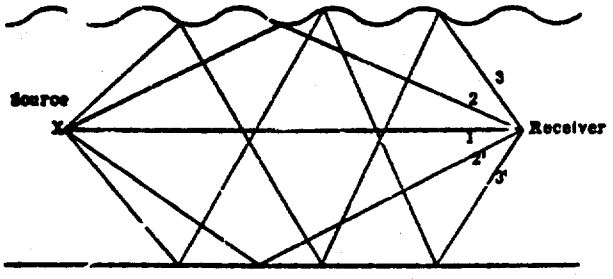

Fig. 4 - Ray Diagram for Direct Radiation Zone

near field, using the boundary loss values reported in this study.

Consider Fig. 4. This diagram can be expected to apply in the region reached by direct radiation, which is essentially free from refraction. It may be seen that there is one ray (1 in the figure) with no boundary contacts, two rays for each order having an equal number of bottom and surface contacts (e.g., 2 and 2'); one ray for each order having one more surface contact than bottom (3) and one ray for each order having one more bottom contact than surface (3'). The set of rays is complete. Accordingly, upper and lower limits on the sound field can be calculated assuming incoherent addition of rays and the following:

I = intensity of direct ray

r_a = surface reflection coefficient

r_b = bottom reflection coefficient.

An upper limit is

$$I + 2I(r_a r_b + r_a^2 r_b^2 + \cdots\cdots)$$
$$+ I(r_a + r_a^2 r_b + \cdots\cdots)$$
$$+ I(r_b + r_a r_b^2 + \cdots\cdots)$$
$$= I\left(1 + \frac{2r_a r_b + r_a + r_b}{1 - r_a r_b}\right) = IK_U.$$

This is an upper limit to the field since it neglects the excess spreading of the higher orders of reflection, and changes of reflection coefficient with angle of incidence. A lower limit can be obtained by considering only the direct arrival and the arrivals having minimum angles of incidence at the boundaries. This is

$$I(1 + 2r_a r_b + r_a + r_b) = IK_L.$$

The loss coefficients of this study may be applied to these results. Table 1 shows the quantities $k_L = 10 \log K_L$ and $k_U = 10 \log K_U$ for the various conditions represented in the study.

Table 1

NEAR FIELD ANOMALY, DB

$k_L = 10 \log K_L$; $k_U = 10 \log K_U$

Frequency (cps)	Sea State 0		Sea State 1		Sea State 2		Sea State 3		Sea State 4		Sea State 5	
	k_L	k_U	k_L	k_U	k_L	k_U	k_L	k_U	k_L	k_U	k_L	k_U
						SAND						
112	6.4	12.3	6.3	11.3	6.3	11.8	6.3	11.8	6.3	11.8	6.3	11.8
446	6.1	10.3	6.1	10.3	6.1	10.3	5.9	9.4	4.7	7.7	4.3	5.4
1120	6.0	10.0	5.8	9.1	5.0	6.7	4.3	5.2	3.9	4.6	3.6	4.1
2820	5.8	9.0	4.1	4.9	3.7	4.3	3.4	3.8	3.0	3.3	2.8	2.8
						MUD						
112	6.3	11.3	6.3	11.3	6.3	11.3	6.3	11.3	6.3	11.3	6.3	11.4
446	5.8	9.1	5.8	9.1	5.8	9.1	5.6	8.3	4.6	5.9	4.3	5.3
1120	5.6	8.2	5.4	7.6	4.5	5.8	3.9	4.6	3.5	4.0	3.4	3.6
2820	4.6	6.1	3.7	4.3	3.3	3.8	3.0	3.3	2.7	2.9	2.7	2.9

There is an exceedingly small amount of data concerning the variability of r_a and r_b with angle of incidence. It is believed that these reflection coefficients decrease rather rapidly with increasing angles of incidence. If this is true, the quantity IK_L might be assumed to be the best representation of the field in the direct radiation zone. For comparative purposes error analyses are presented later using both k_L and k_U. This near-field correction can not, of course, be applied in close proximity to the source, since the intensity of the reflected waves is overestimated for small separations between source and receiver. For practical purposes the near field in shallow water can be regarded as covering ranges out to about 1000 yards. Accordingly, Eqs. (4A), (4B), and (4C) should be modified to read:

$$N_w = 20 \log_{10} R + aR + 60 - k_L \text{ (db)} \qquad 1 \leq R \leq H \qquad (4A)'$$

$$= 15 \log_{10} R + aR + a_T \left(\frac{R}{H} - 1\right) + 5 \log_{10} H + 60 - k_L \text{ (db)} \qquad 8H \geq R \geq H \qquad (4B)'$$

$$= 10 \log_{10} R + aR + a_T \left(\frac{R}{H} - 1\right) + 10 \log_{10} H + 64.5 - k_L \text{ (db)} \qquad R \geq 8H. \qquad (4C)'$$

OTHER MODES OF PROPAGATION

The foregoing description applies to the propagation situation which occurs most of the time off the East Coast of the United States. Internal channels were observed so seldom that they were not considered an important situation in our analysis. Presumably, the surface and bottom do not affect this propagation mode which is explicable in terms of spreading and temperature absorption losses. This mode is known to be important in certain localities such as the Scotian Shelf. Very little effect was found with respect to source and receiver depths.

No attempt was made to carry the analysis below 100 cps. This frequency has a wavelength about a quarter of the water depth of 200 feet, typical of these measurements. Undoubtedly a ray picture does not apply here and normal mode theory is required to explain the observations. Another phenomenon associated with low frequencies which was not treated here was propagation from one point to another by way of the sub-bottom or the seismic mode. The existence of this path has definitely been established, and can be of importance at longer ranges and lower frequencies.

This analysis is not applicable to bottoms with sustained slopes in which a ray picture accounting for progressively changing limiting angles must be employed. The shallow-water analysis applies up to depths of 100 fathoms, which occur at about 100 miles from shore.

In the transition region between shallow water and deep water, it is known that propagation may be described quite well in terms of a detailed ray analysis.

PREDICTION OF SHALLOW-WATER ACOUSTIC PARAMETERS

A method is presented below for the estimation of the statistical distributions of propagation loss N_w in shallow water. Equations are given for determining the average values of quantities and tables for the associated problem errors.

Mean Values

Propagation loss is given as functions of the variables which follow. The range of validity of the variables is indicated.

R	Range in kiloyards	(0-100)
f	Frequency in kilocycles per second	(0.1-2.8)
D	Water depth in feet	(100-600)
	Bottom type	(sand or mud)
L	Layer depth in feet	(0-600)
S	Sea state	(0-5)
h	Wave height in feet	
H	Skip distance in kiloyards	
a_s	Surface loss, db/bounce	
a_b	Bottom attenuation factor, db/bounce	
a_T	Attenuation factor, db/bounce	
a	Absorption coefficient, db/kyd	
k_L	Near Field Anomaly, Lower Limit, db	
k_U	Near Field Anomaly, Upper Limit, db	

In terms of these symbols, the following equations hold for mean value

$$N_w = 20 \log_{10} R + aR + 60\ (db) - k_L^* \qquad R \leq H \qquad (4A)'$$

$$= 15 \log_{10} R + aR + a_T\left(\frac{R}{H} - 1\right) + 5 \log_{10} H + 60\ (db) - k_L^* \qquad 8H \geq R \geq H \qquad (4B)'$$

$$= 10 \log_{10} R + aR + a_T\left(\frac{R}{H} - 1\right) + 10 \log_{10} H + 64.5\ (db) - k_L^* \qquad R \geq 8H \qquad (4C)'$$

where

$$H = \sqrt{\frac{L + D}{8}}\ \text{kyd}$$

$$a = 0.01\ f^2 \text{ approximately.}$$

$$a_T = -10 \log_{10} [r_b r_s + r_b^2 (1 - r_s)]$$

* or k_U

$$a_s = -10 \log_{10} r_s$$

$$= 1.59 \sqrt{fh}, \quad fh \geq 4.14$$

$$= 10 \log_{10} \left[1 + \left(\frac{fh}{4.14} \right)^4 \right] \quad fh \leq 4.14$$

$a_b = -10 \log_{10} r_b$, a function of bottom type

$$k_L = 10 \log_{10} (1 + 2 r_s r_b + r_s + r_b)$$

$$k_U = 10 \log_{10} \left(1 + \frac{2 r_s r_b + r_s + r_b}{1 - r_s r_b} \right)$$

The quantities a_s and a_b are displayed in Figs. 3 and 5, respectively; a_v is displayed in Figs. 6-11.

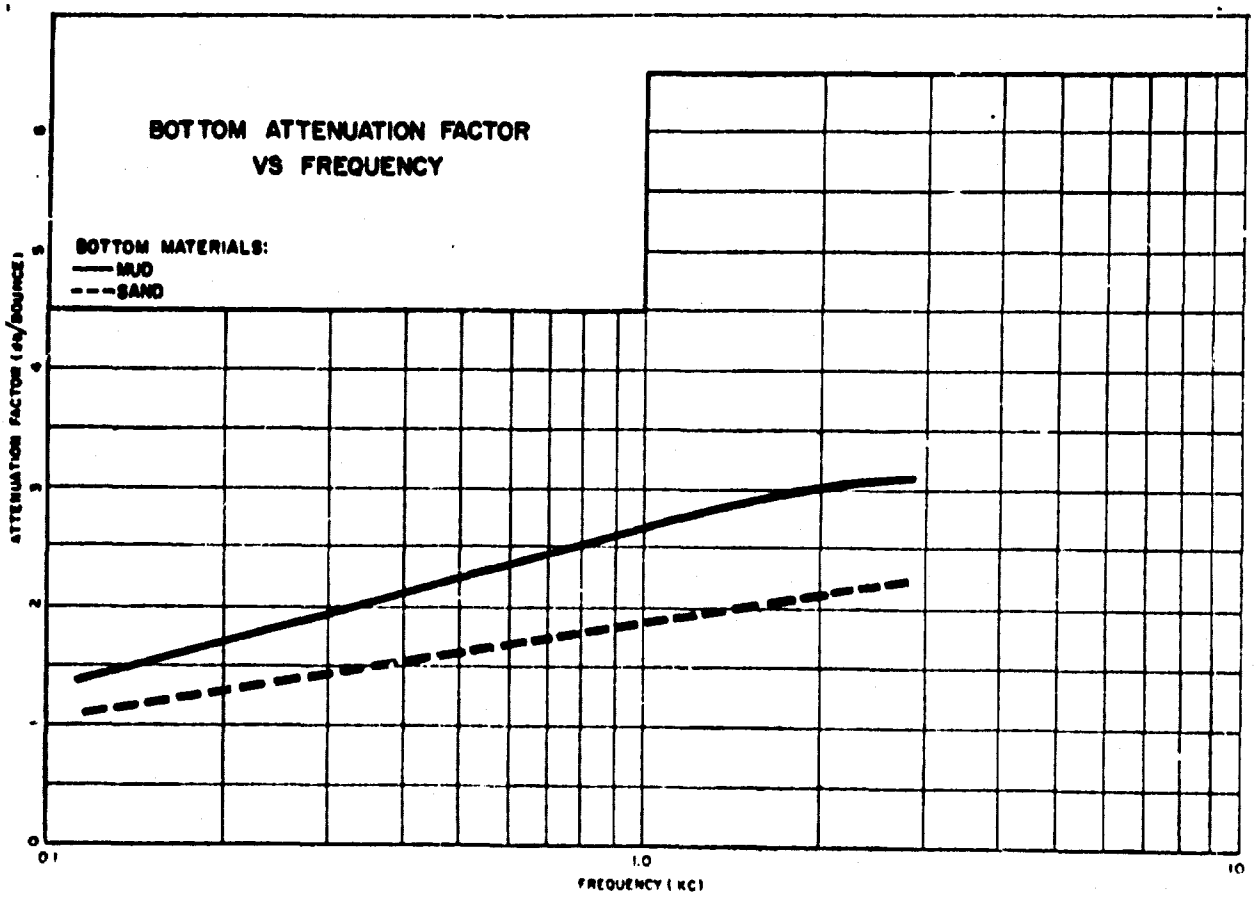

Fig. 5 - Bottom Attenuation Factor vs Frequency

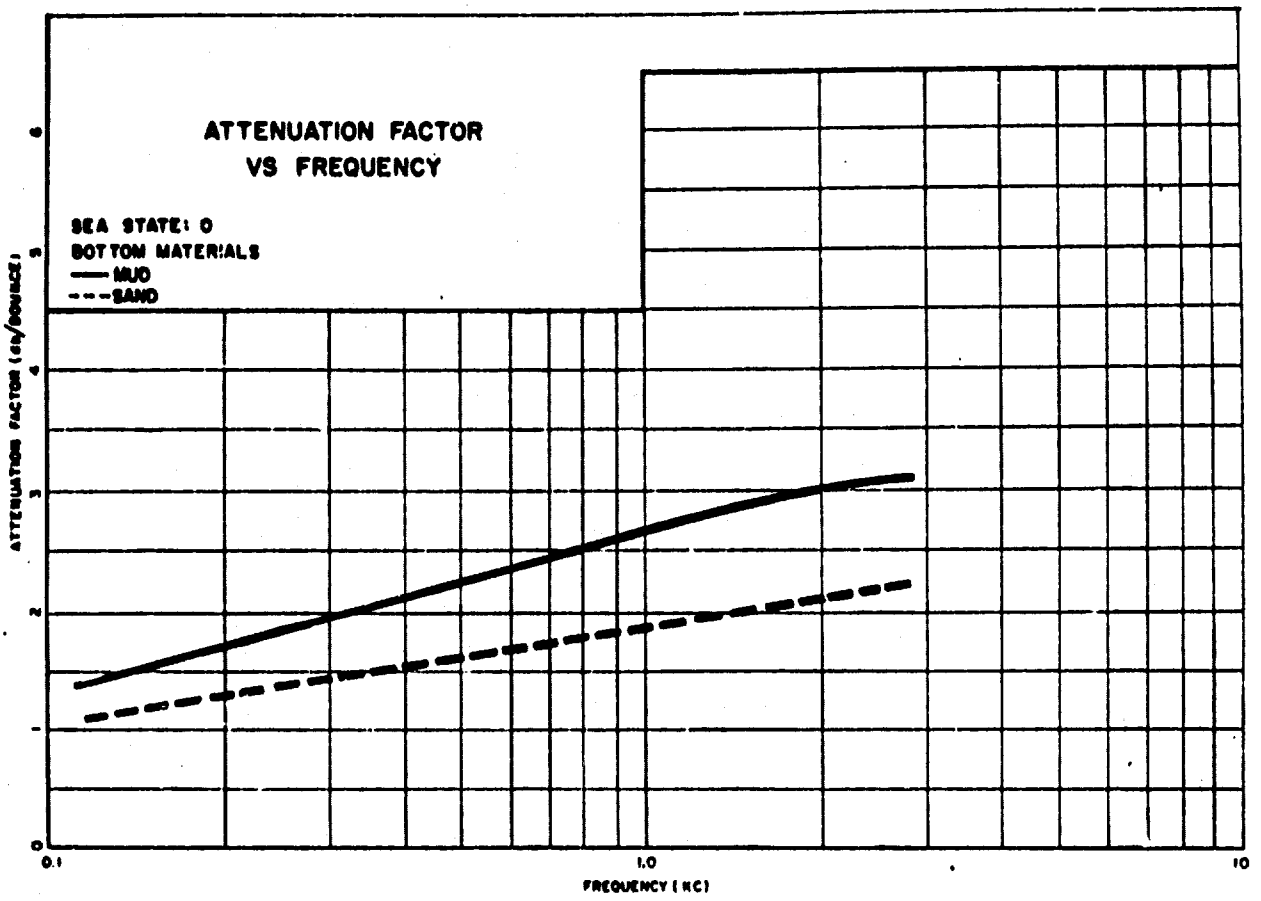

Fig. 6 - Attenuation Factor vs Frequency for Sea State 0

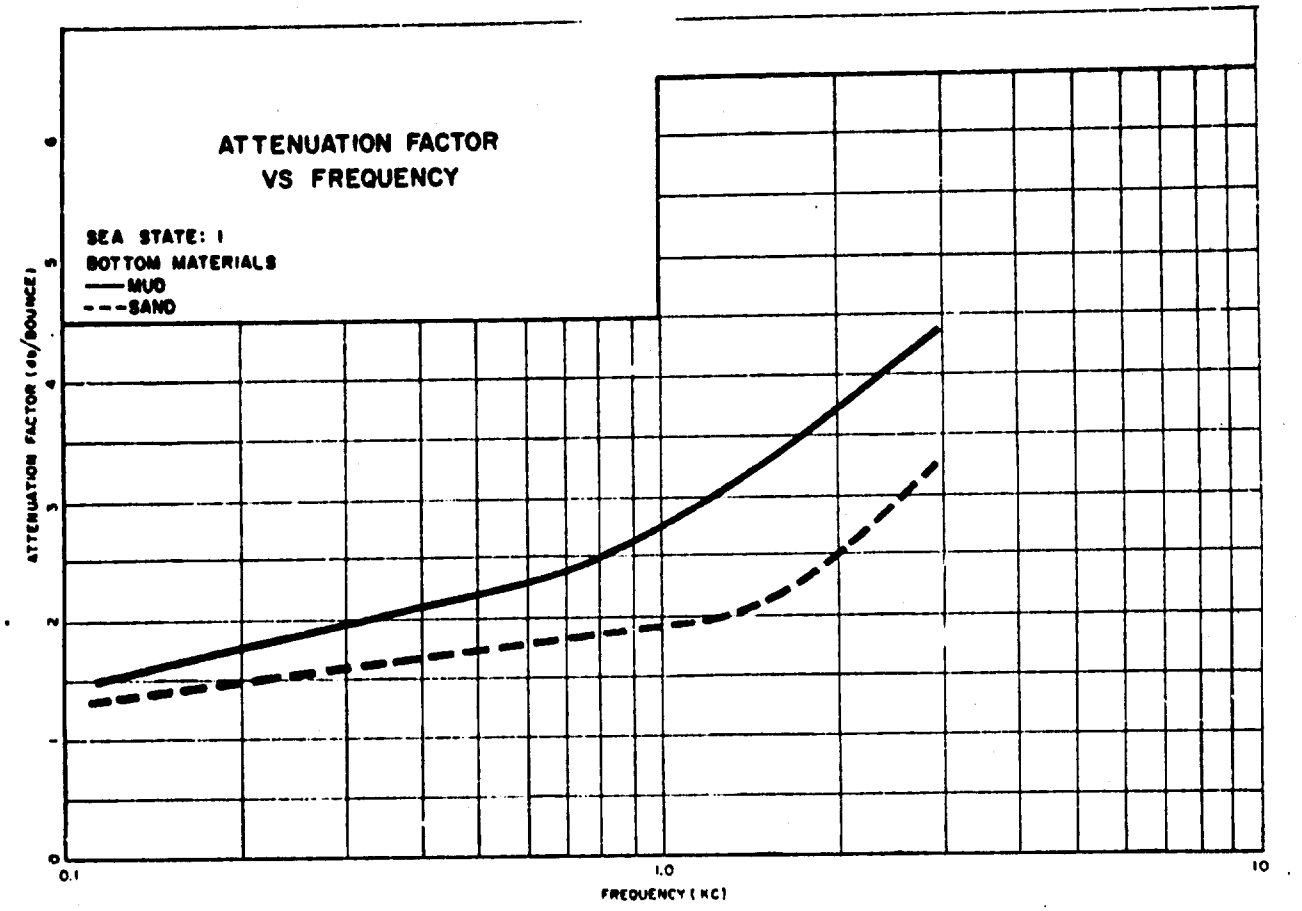

Fig. 7 - Attenuation Factor vs Frequency for Sea State 1

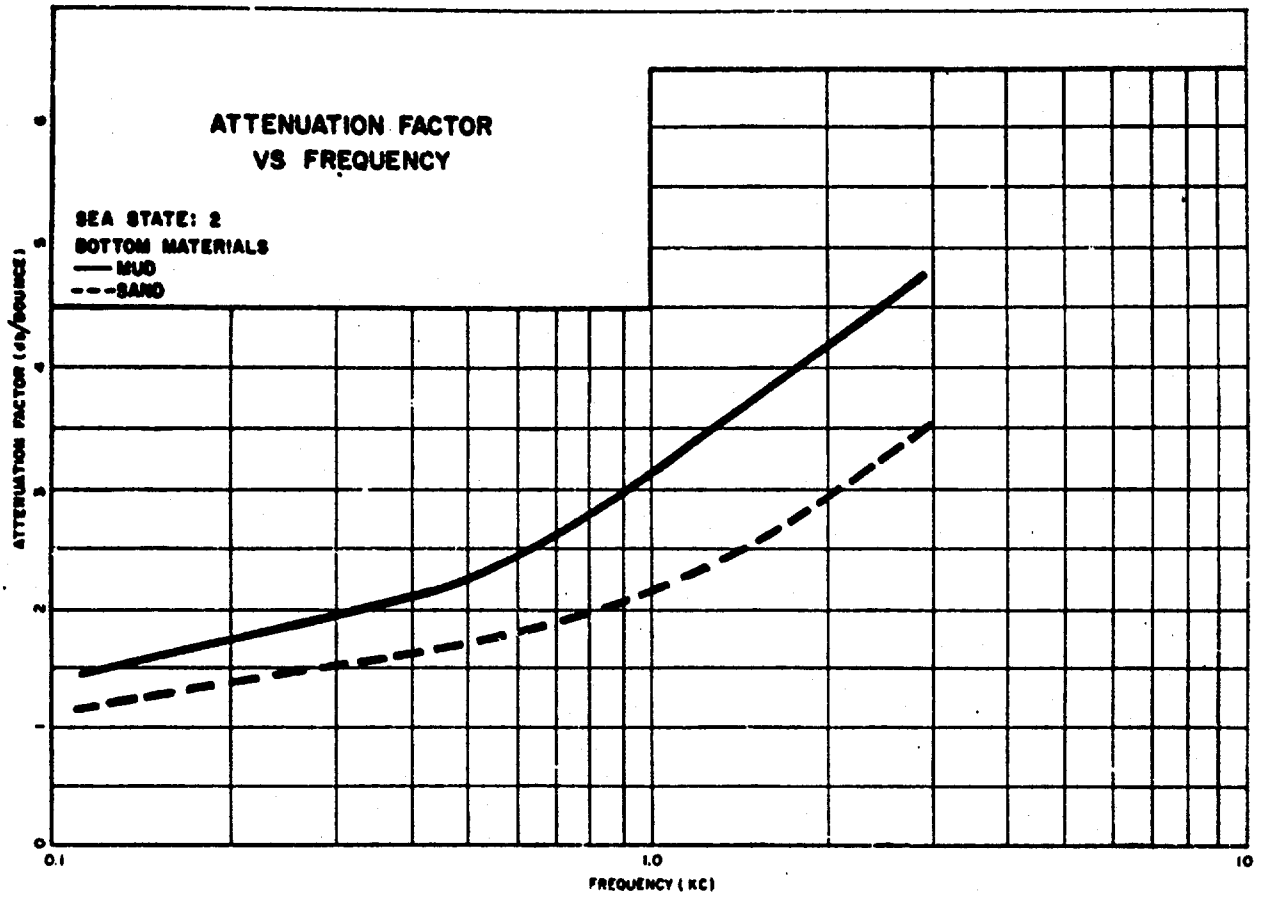

Fig. 8 - Attenuation Factor vs Frequency for Sea State 2

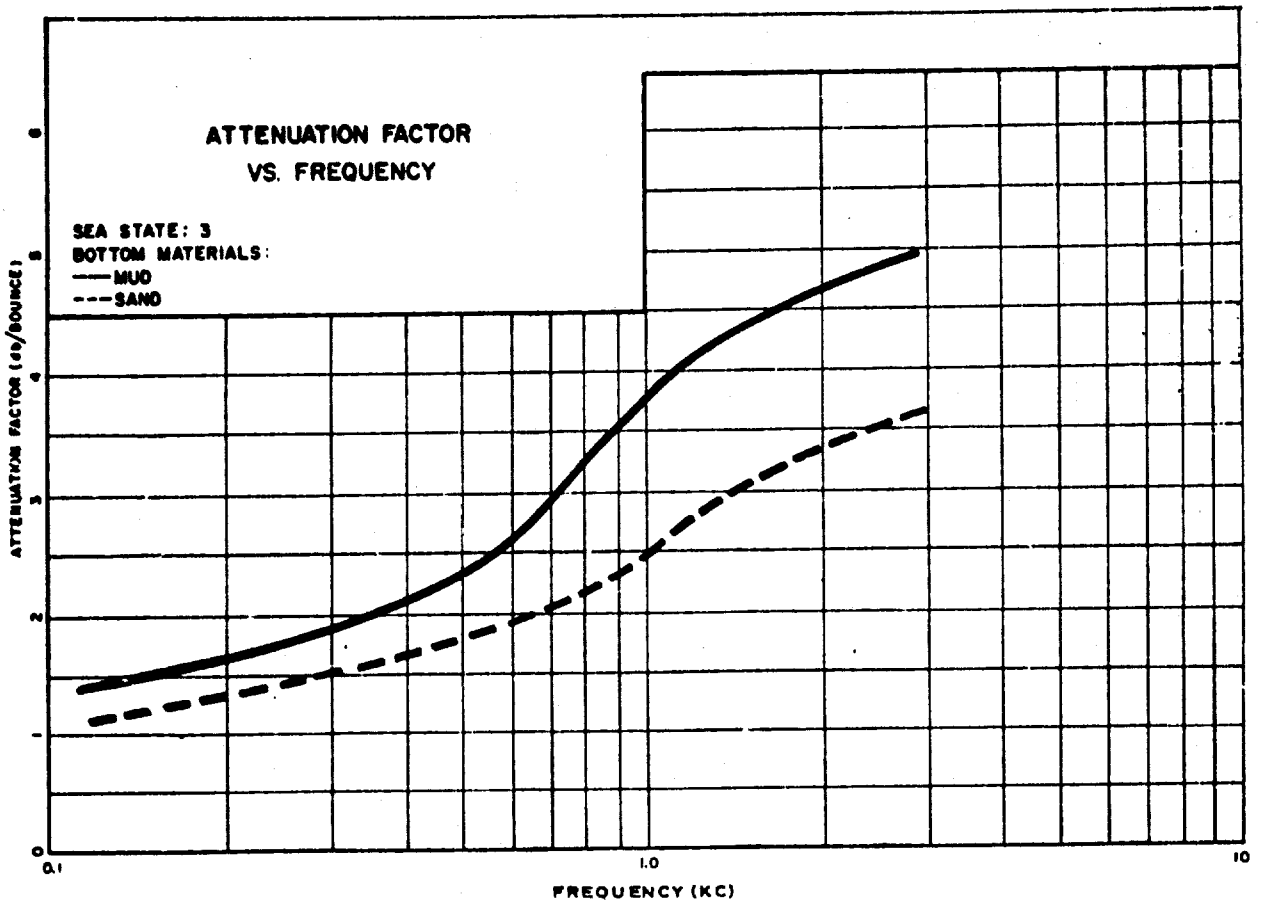

Fig. 9 - Attenuation Factor vs Frequency for Sea State 3

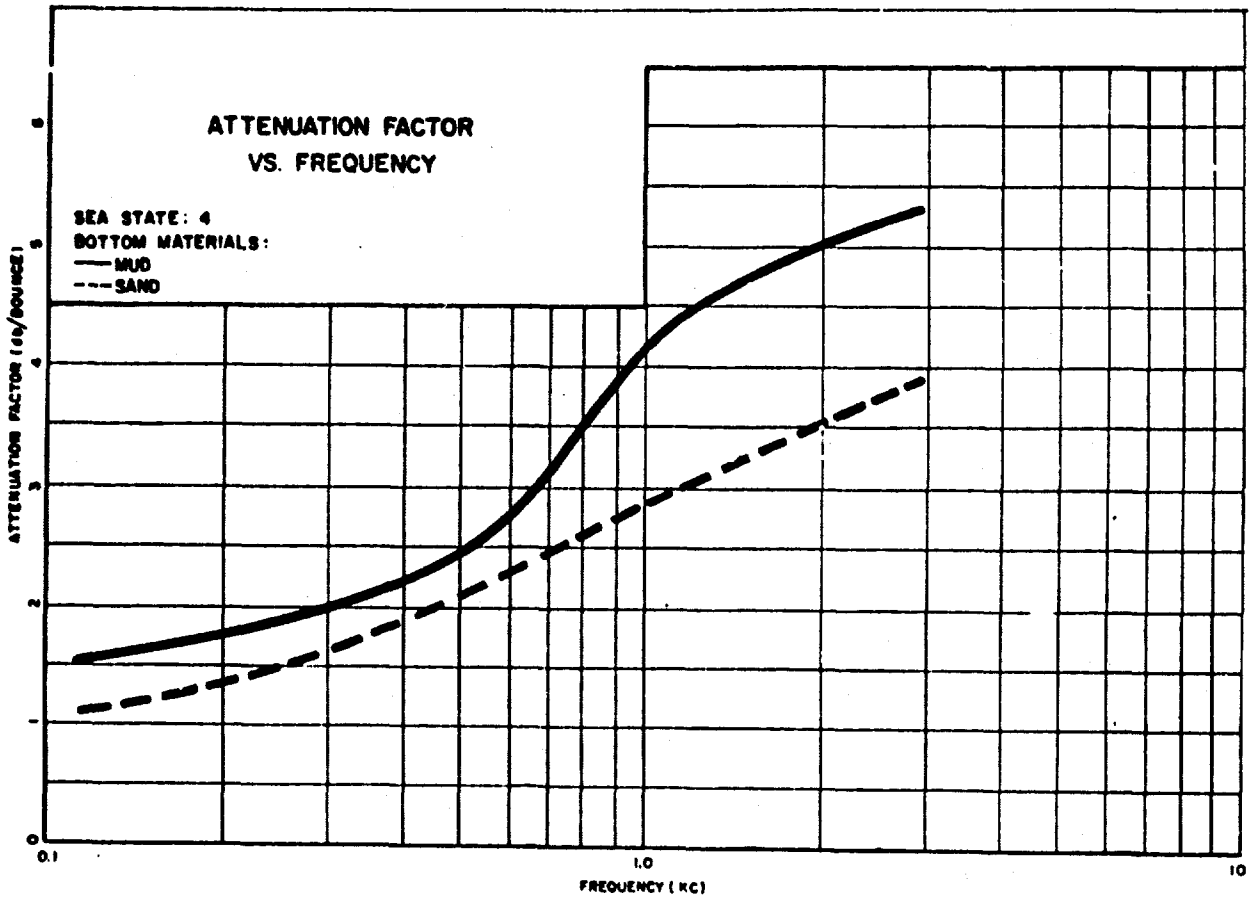

Fig. 10 - Attenuation Factor vs Frequency for Sea State 4

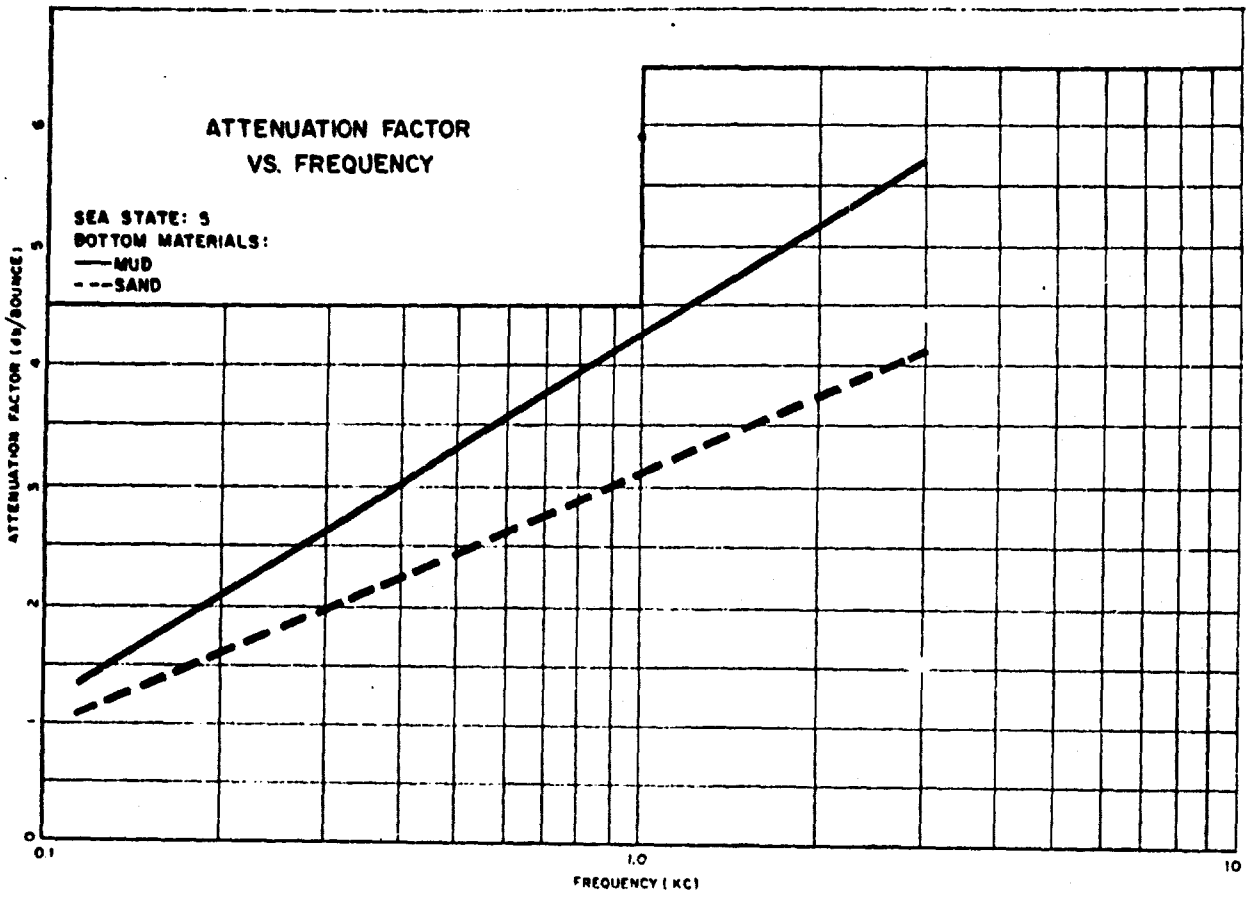

Fig. 11 - Attenuation Factor vs Frequency for Sea State 5

Error Analysis

An error analysis was made based on References (1), (2), and (10) in Table 4, p. 27, since these contain a large portion of the data and represent a reasonable cross-section of environmental conditions. The analysis was carried out at frequencies of 112, 446, 1120, and 2820 cps and ranges of 3, 9, 30, 60, and 90 kyd. For each document-frequency-range combination, approximately 30 propagation values were picked at random. These are called N_w. Corresponding to each such value, a value (N_{wo}) was computed using Eqs. (4A)', (4B)', (4C)', and the near-field correction k_L. The differences, or anomalies $N_A = N_w - N_{wo}$, were computed. Table 2 shows the distribution of N_A at each range and frequency.

Table 2

DISTRIBUTION OF N_A

Range (kyd)	3	9	30	60	90
		112 cps			
Upper Quartile	-1	-1	5	7	5
Median	-3	-4	-5	-3	-3
Lower Quartile	-6	-7	-13	-10	-11
Interquartile Range	5	6	18	17	16
Number of Observations	67	72	74	70	60
		446 cps			
Upper Quartile	0	2	12	7	4
Median	-3	-5	-4	-4	-4
Lower Quartile	-7	-11	-15	-14	-19
Interquartile Range	7	13	27	21	23
Number of Observations	92	107	105	107	93
		1120 cps			
Upper Quartile	2	5	17	9	5
Median	-2	-1	-2	-1	-7
Lower Quartile	-6	-6	-16	-12	-20
Interquartile Range	8	11	34	21	25
Number of Observations	92	108	103	108	78
		2820 cps			
Upper Quartile	2	7	14	2	3
Median	-1	2	2	-6	-9
Lower Quartile	-6	-6	-8	-17	-17
Interquartile Range	12	13	22	19	14
Number of Observations	90	100	97	86	70

Note: The above values were obtained using the following values for k_L:

112	7
446	6
1120	5
2820	4

Table 3

DISTRIBUTION OF N_A'

Range (kyd)	3	9	30	60	90
		112 cps			
Upper Quartile	3	5	8	12	10
Median	0	0	2	0	1
Lower Quartile	-4	-3	-3	-5	-6
Interquartile Range	7	8	11	17	16
Number of Points	45	84	92	82	68
		446 cps			
Upper Quartile	2	4	7	13	6
Median	-1	0	0	-3	-6
Lower Quartile	-4	-6	-10	-10	-17
Interquartile Range	6	10	17	23	23
Number of Points	62	101	129	120	101
		1120 cps			
Upper Quartile	2	5	20	16	6
Median	-2	0	5	5	-5
Lower Quartile	-6	-5	-8	-11	-17
Interquartile Range	8	10	28	27	23
Number of Points	63	110	127	110	85

References (1), (2), (10), (18), and (19)
Near Field Anomaly = k_U

A similar analysis was carried out using the near-field correction factor k_U instead of k_L. In this case all available data from References (1), (2), (10), (18), and (19) in Table 4 were used for the frequencies 112, 446, and 1120 cps and ranges 3, 9, 30, 60, and 90 kiloyards. The anomalies N_A' in this case are defined as

$$N_A' = N_w - N_{we}'$$

where N_{we}' is the predicted propagation loss using k_U. The results are shown in Table 6.

For 112 and 446 cps, the results of Table 3 show a better average fit of the prediction equations to the data than does Table 2. For 1120 cps the results of the two tables are comparable. On the average the interquartile ranges of Table 3 are less than the interquartile ranges of Table 2.

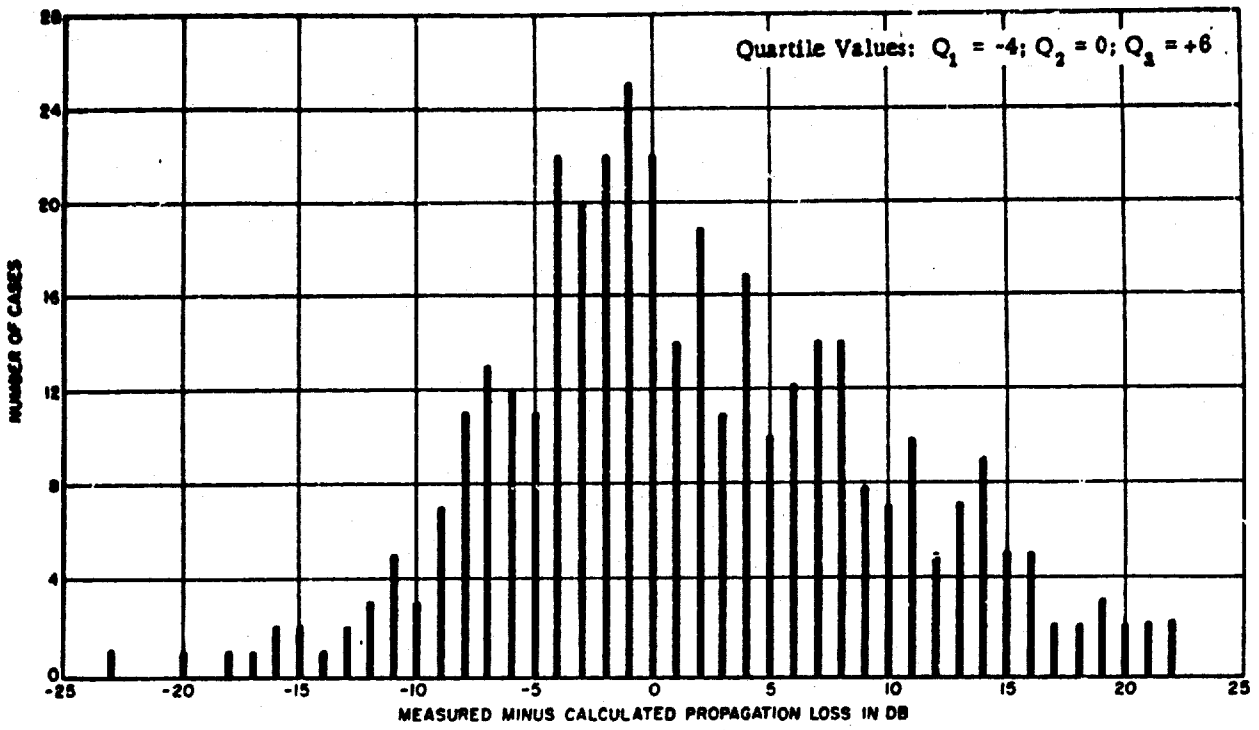

Fig. 12A - 112 cps

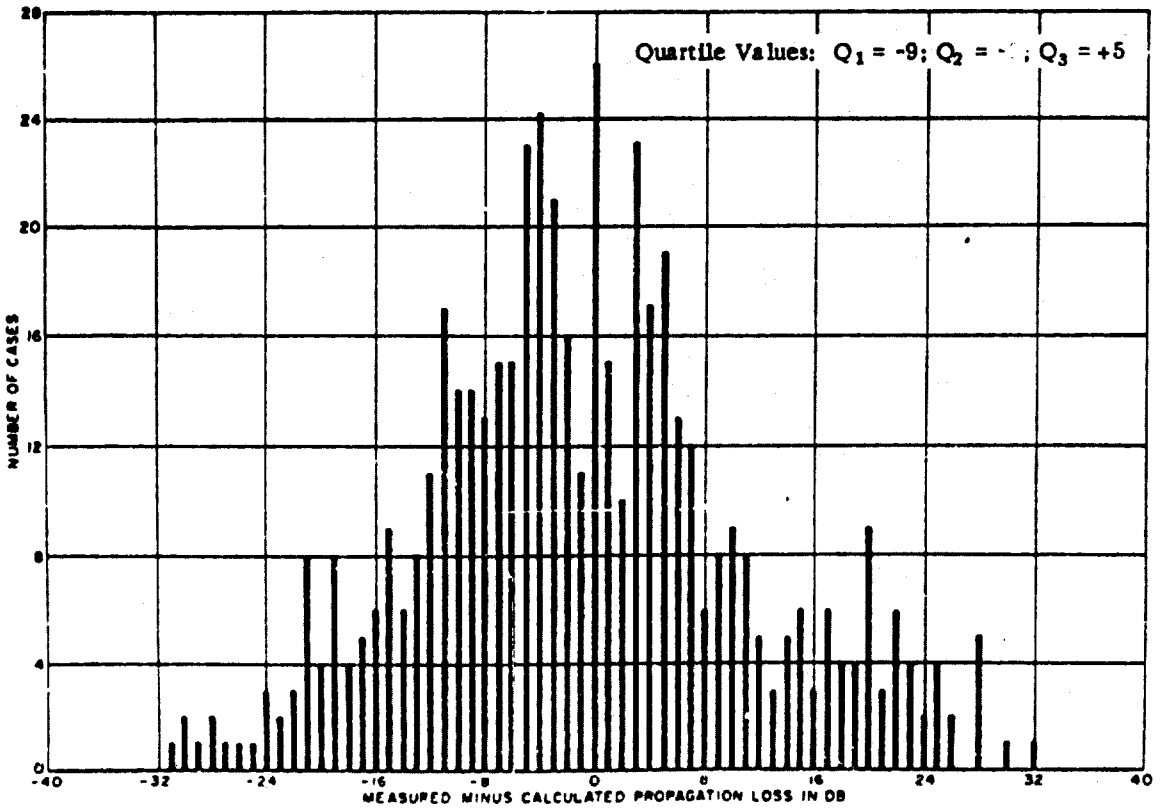

Fig. 12B - 446 cps

Fig. 12 - Distributions of Propagation Loss Anomaly

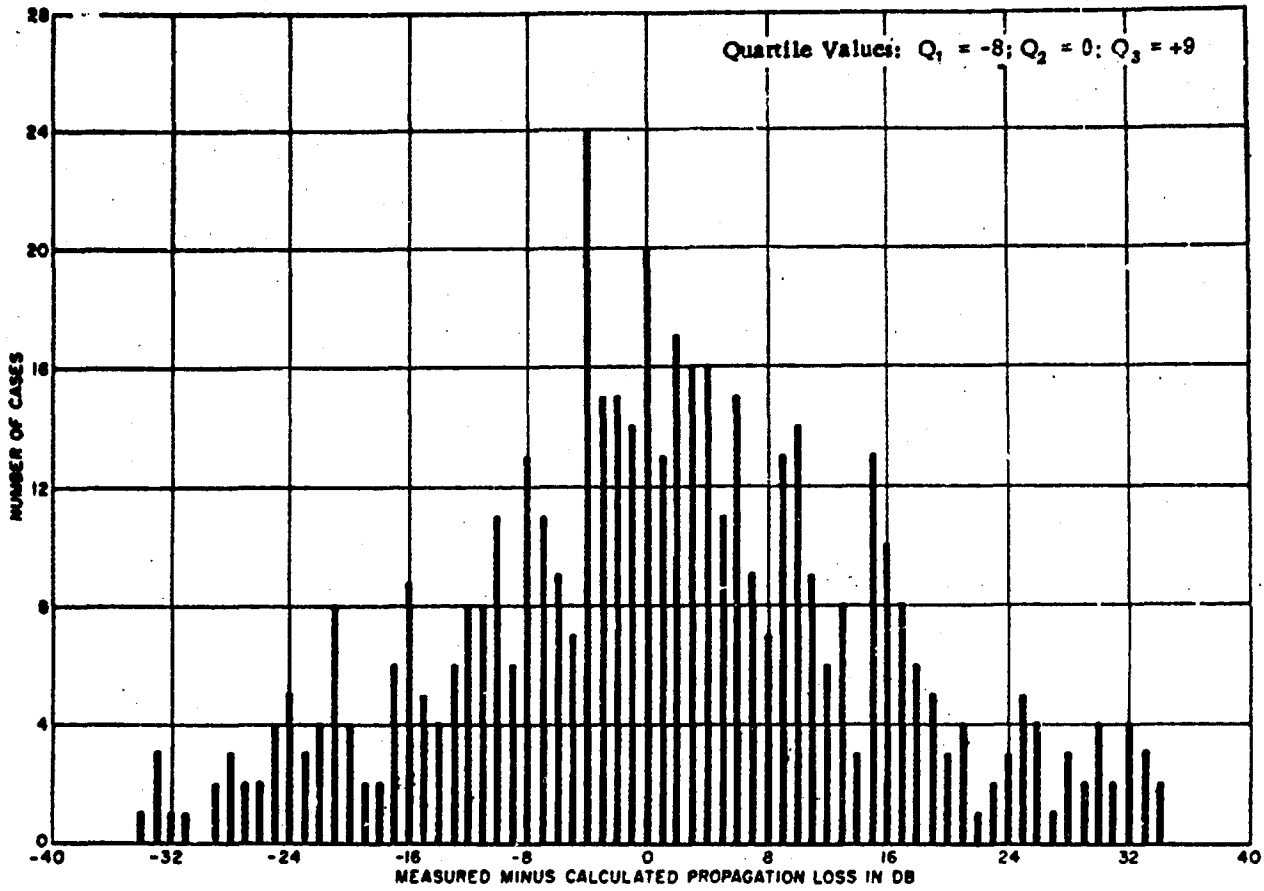

Fig. 12C - 1120 cps

Fig. 12 (Cont'd) - Distributions of Propagation Loss Anomaly

Distributions of the propagation anomaly, N_A, were computed for the frequencies 112, 446, and 1120 cps for the ranges 3, 9, 30, 60, and 90 kiloyards combined. These are shown in Fig. 12. The interquartile ranges are larger than might be desired. One reason for this could be the variability in the source level of the explosives and another is the inevitable bias of data due to lack of homogeneity. Thus, there are fewer measured values at the longer ranges, because the field is sometimes too weak to be measured. Thus, unweighted averages show a trend toward apparently unpredictable strong fields at the longer ranges. These fields are probably due in part to other modes of propagation, principally seismic. The analysis and prediction data presented herein are valid for values of estimated propagation loss less than about 135 db. Scatter diagrams were prepared to show the variability of the measured loss with the predicted propagation loss. These appear as Figs. 13A, 13B, and 13C.

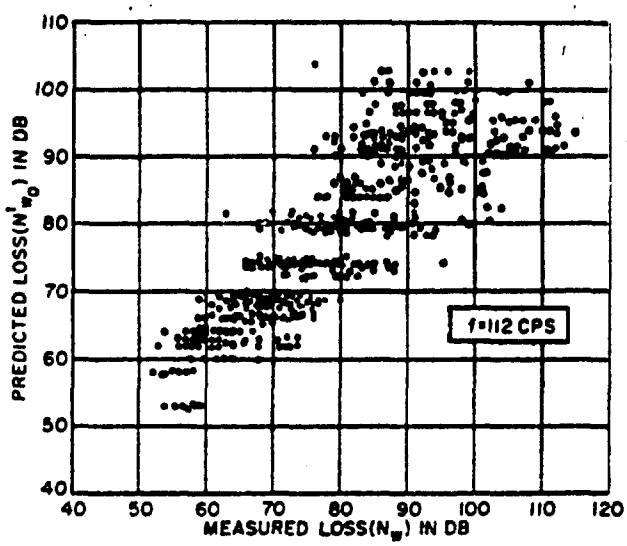

Fig. 13A - 112 cps

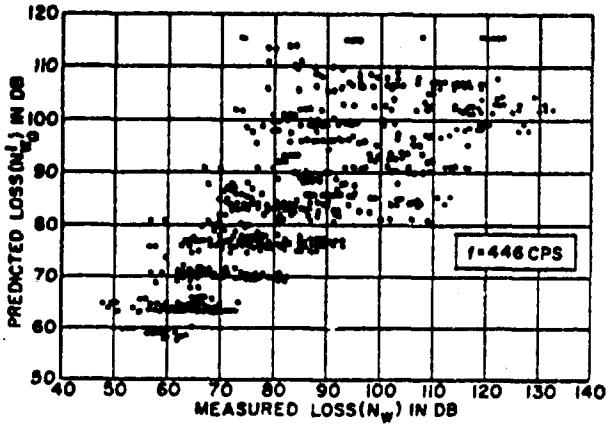

Fig. 13B - 446 cps

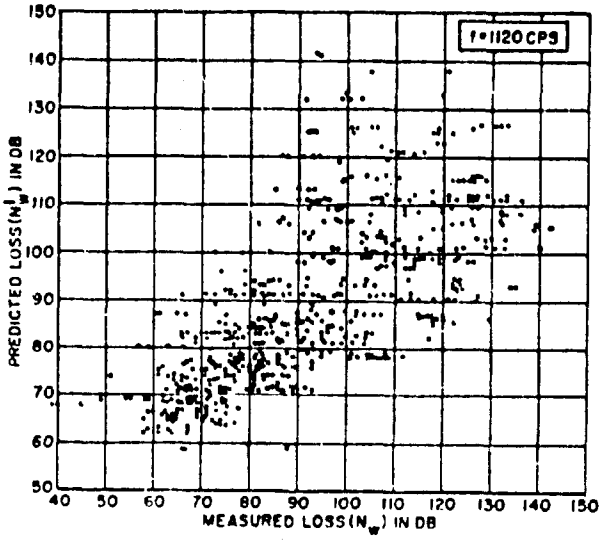

Fig. 13C - 1120 cps

Fig. 13 - Scatter Diagram—Predicted vs Measured Loss

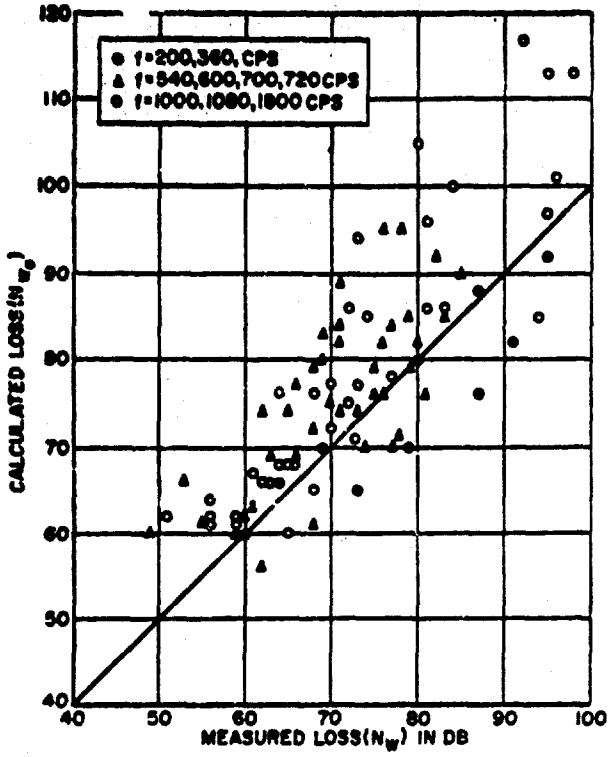

Fig. 14 - Predicted vs Measured Loss Using k_L for Sinusoidal Sources

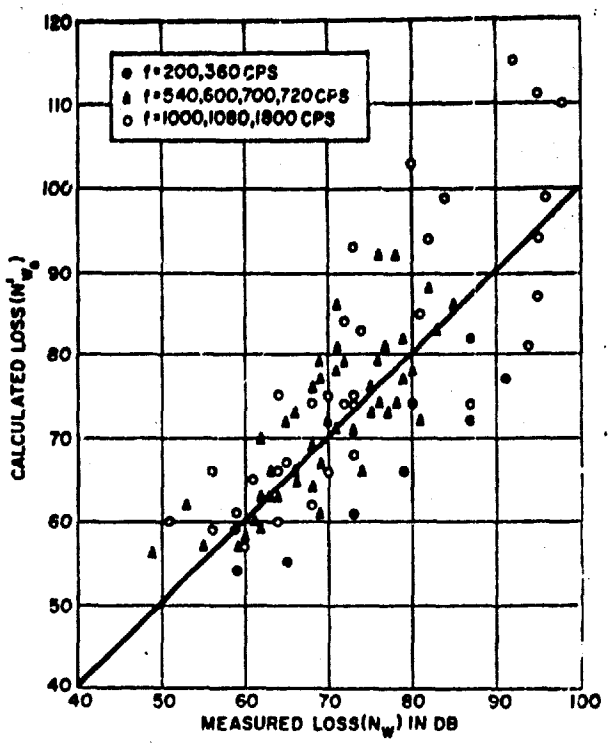

Fig. 15 - Predicted vs Measured Loss Using k_U for Sinusoidal Sources

To further compare the goodness of fit of the prediction equations when using both near-field correction factors, k_L and k_U, a scatter diagram was constructed of data obtained from all available shallow-water propagation measuremens made using calibrated sinusoidal acoustic generators as acoustic sources. These scatter plots are shown in Figs. 14 and 15. In both the explosive results shown in Tables 5 and 6 and the sinusoidal measurements shown in Figs. 14 and 15, the prediction equations fit the measurements better when k_U rather than k_L is employed.

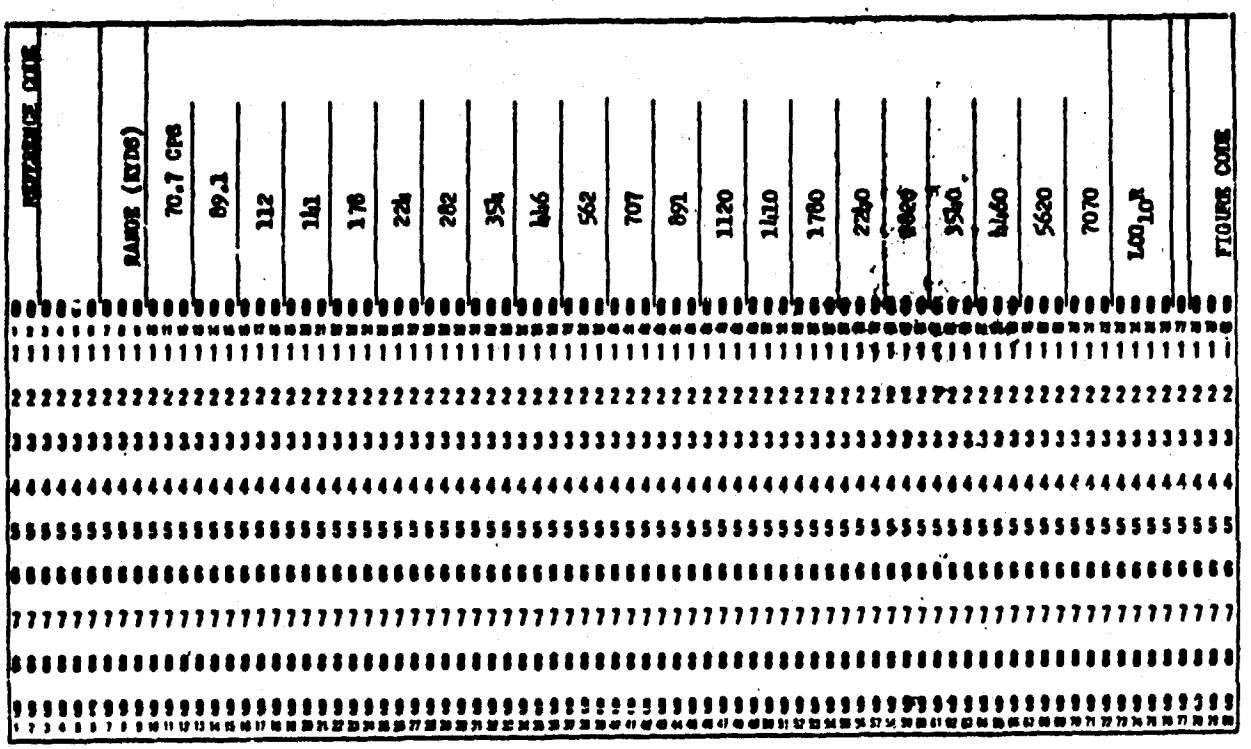

Fig. 16 - Acoustic Data Card Layout

SUMMARY SHEET OF ACOUSTIC SOURCE PARAMETERS

Reference No. _____ Document No. _____ Date Of Cruise _____

RUN NO.	FIGURE NO.	HYD DEPTH (FT)	SOURCE DEPTH (FT)	BOTTOM DEPTH (FT)	BOTTOM MATERIAL	RANGE (KYDS)	SOUND SOURCE	SEA STATE	LOCATION

Fig. 17 - Summary Sheet of Acoustic Source Parameters

Summary of Acoustic Data

The acoustic data sources were available in the form of documents and/or IBM cards. Table 4 shows a complete list of all sources received. Not all of the data contained in these sources were usable. For this study, propagation loss data with a minimum range of the order of 3000 yards were required, with sampling done at 1000-yard increments thereafter. The maximum frequency of interest was 7070 cps. These specifications eliminated from use three-fourths of the approximately 22,000 IBM cards received. For example, in References (5), (6), and (7) propagation-loss data are given in range increments of 200 to 250 yards. Hence, only every fifth card was used. Some cards were also omitted because the frequencies were greater than 7070 cps. Similarly, some cards from Reference (16) were omitted because the minimum range was greater than 7000 yards.

Table 4

LIST OF PROCESSED ACOUSTIC DATA SOURCES

Ref. No.	No. of Runs	No. of Freq's	Average No. of Ranges/Graph	Number of Cards	Received as Document (D) or IBM Cards
(1)	6	9	45	1,501	D
(2)	9	9	54	2,170	D
(3)	2	10	60	239	D
(4)	7	10	40	558	D
(5)	9	10	38	676	IBM
(5)					IBM
(6)	8	10	45	673	IBM
(7)	10	10	29	522	IBM
(8) and (9)	30	3	4	137	IBM
(10)	10	8	53	2,178	D
(11)	26	4	6	4,076	IBM
(12)	18	4	13	490	D
(15)	6	8	57	349	D
(16)	--	--	--	--	IBM
(17)	1	8	21	21	IBM
(18)	6	6	52	615	D
(19)	5	6	47	862	D
			Total	15,067	

All the propagation-loss data derived from the acoustic data sources were transcribed into workable IBM Acoustic Data Cards, the layout of which is shown in Fig. 16. Columns 1 and 2 contain codes for identification of the reference documents listed at the end of this section. Columns 7 to 9 list range in kiloyards, while columns 73 to 76 show the common logarithm of this range. Columns 10 to 72 list propagation loss according to frequency bands. Columns 78 to 80 provide identification of acoustic data in the references. Columns 3, 4, 5, 6, and 77 are reserved for future use.

The Acoustic Data Cards are supplemented with Summary Sheets of Acoustic Source Parameters. The latter have been classified as oceanographic, mechanical, and seasonal, and are shown in the Summary Sheets arranged according to runs. A copy of a Summary Sheet is shown in Fig. 17. A summary of the locations and of the pertinent reference numbers is listed in Table 5.

Table 5

GEOGRAPHICAL LOCATION OF PROCESSED ACOUSTIC DATA SOURCES

Location	Reference Numbers
Long Island - Nantucket	(1) and (2)
Long Island - Nantucket	(3) and (5)
Greenland	Part of (4)
Iceland - Faeroe Islands	Part of (4)
Long Island - Nantucket	(6), (7), and part of (10)
Nova Scotia	Part of (10)
Fishers Island	(8)
Block Island	(9)
South Carolina - Florida	(12)
Western North Atlantic	(15), (18), and (19)
South Carolina	(17)

Table 6

REPORTED FREQUENCIES IN EACH REFERENCE

REF	FIG PER REF \ FREQ.	70.7	89.1	112	141	178	224	202	354	446	562	707	1120	1410	1780	2240	2820	3540	4460	5620	7070	CARDS PER REF
(1)	34	x	x	x				x		x		x	x		x		x					1501
(2)	41	x	x	x				x		x		x	x		x		x					2170
(3)	4			x			x				x		x	x	x		x		x	x	x	239
(4)	14			x			x				x		x	x	x		x		x	x	x	558
(5)	18			x			x				x		x	x	x		x		x	x	x	676
(6)	15			x			x				x		x	x	x		x		x	x	x	673
(7)	18			x			x				x		x	x	x		x		x	x	x	522
(8)	8										x										x	46
(9)	22										x				x						x	91
(10)	42		x	x		x		x		x		x	x				x					2178
(11)	765					x					x				x						x	4076
(12)	39	x						x					x					x				490
(15)	6			x		x		x	x	x	x	x	x									349
(17)	1			x		x		x	x	x	x	x	x									21
(18)	12			x				x		x		x	x		x							615
(19)	18			x				x		x		x	x		x							862
	CARDS PER FREQ.	4246	5385	8159	267	3513	2515	9338	740	5448	4335	6653	1029	2427	8655	278	6805	455	2432	2102	4902	

CONCLUSIONS

a. Bottom loss in deep and shallow water are compatible. Differences can be attributed to steeper angles of the deep water rays. Bottom loss over mud is appreciably higher than over sand.

b. Surface scattering is the same for deep and shallow water.

c. There is a strong surface-bottom coupling in shallow-water propagation, such that the propagation losses are controlled by the number of contacts with both surfaces. The surface scatters the rays, whereas the bottom absorbs them.

d. The thermal structure of the water affects the propagation through its influence on skip distance and the number of surface and bottom contacts.

e. The distribution of sea states in shallow water (100 fathoms) appears to be quite different from that in deep water.

f. On the average, propagation loss is independent of source and receiver depths.

RECOMMENDATIONS

a. Improve analytical model.

b. Obtain a more detailed picture of the loss mechanisms, a_B and a_s and their interdependence. Include analytical treatment and specialized measurements. For example: (1) obtain a better model of surface-bottom interactions through a transport type of phenomenological model; (2) make direct measurement of bottom loss at small grazing angles; and (3) determine the angular dependence for both a_B and a_s.

c. To the extent that further measurement programs are established, it is recommended that the coverage of environmental conditions be completed with rough water measurements in summer and propagation measurements over mud bottoms in winter.

ABSTRACT CARD LAYOUT

SND-USNUSL-232

Navy Underwater Sound Laboratory
Report No. 550
COLOSSUS II SHALLOW-WATER ACOUSTIC PROPAGATION STUDIES, 1 June 1962, i-iii + 30pp., figs.
UNCLASSIFIED

Project Colossus II was established in 1954 to investigate acoustics in shallow water (150 fathoms or less). A portion of that program was devoted to a study of underwater acoustics propagation. The frequency range of interest was 100 to 3000 cps.

Presented in this report are the results of the acoustic propagation loss studies, which include a summary of the analysis and a prediction method of estimating the statistical distribution of propagation loss.

1. Shallow water sound—Propagation

I. COLOSSUS II
II. SS046002-8037

1. Shallow water sound—Propagation

I. COLOSSUS II
II. SS046002-8037

Navy Underwater Sound Laboratory
Report No. 550
COLOSSUS II SHALLOW-WATER ACOUSTIC PROPAGATION STUDIES, 1 June 1962, i-iii + 30pp., figs.
UNCLASSIFIED

Project Colossus II was established in 1954 to investigate acoustics in shallow water (150 fathoms or less). A portion of that program was devoted to a study of underwater acoustics propagation. The frequency range of interest was 100 to 3000 cps.

Presented in this report are the results of the acoustic propagation loss studies, which include a summary of the analysis and a prediction method of estimating the statistical distribution of propagation loss.

1. Shallow water sound—Propagation

I. COLOSSUS II
II. SS046002-8037

1. Shallow water sound—Propagation

I. COLOSSUS II
II. SS046002-8037

INITIAL DISTRIBUTION LIST

ONR, Code 411
" " 466
" " 492
" London Branch (8)
OpNav (Op-095B)
" (Op-03EG)
" (Op-31)
" (Op-32)
" (Op-07T) (2)
" (Op-71)
BuShips, Code 320
" " 333
" " 335 (3)
" " 340
" " 342C
" " 351
" " 370
" " 670
" " 671D
" " 681A
" " 688
" " 689B
" " 689D

BuWeps, Code R-56
ComOpTevFor, Undersea Warfare Division
CO, USNUOS, Newport
CO and Dir., USNEL
CO, US Navy Mine Defense Laboratory
Com, NADC
" NOL
" US NOTS, China Lake
" US NOTS, Pasadena Annex
Dir., NRL
" ORL
" WHOI
Dir., Marine Physical Laboratory Scripps Institution of Oceanography
Commander, New York NavShpyd (Code 109)
Dir., Systems Analysis Group, R and D Planning Council, NOL
Dir., Weapons System Evaluation Group
Committee on Undersea Warfare National Research Council
ASTIA, Document Service Center (10)

UNCLASSIFIED

UNCLASSIFIED